

Article

Stress Corrosion Cracking of an Austenitic Stainless Steel in Nitrite-Containing Chloride Solutions

R. K. Singh Raman ^{1,*} and Wai Hoong Siew ²

¹ Department of Mechanical and Aerospace Engineering, Monash University, Melbourne, Victoria 3800, Australia

² Mechanical Engineer, IBM Australia, 60 City Road, Melbourne, Victoria 3006, Australia; E-Mail: whs6211@gmail.com

* Author to whom correspondence should be addressed; E-Mail: raman.singh@monash.edu; Tel.: +61-3-9905-3671.

External Editor: Fuhui Wang

Received: 3 June 2014; in revised form: 28 September 2014 / Accepted: 4 November 2014 /

Published: 5 December 2014

Abstract: This article describes the susceptibility of 316L stainless steel to stress corrosion cracking (SCC) in a nitrite-containing chloride solution. Slow strain rate testing (SSRT) in 30 wt. % MgCl₂ solution established SCC susceptibility, as evidenced by post-SSRT fractography. Addition of nitrite to the chloride solution, which is reported to have inhibitive influence on corrosion of stainless steels, was found to increase SCC susceptibility. The susceptibility was also found to increase with nitrite concentration. This behaviour is explained on the basis of the passivation and pitting characteristics of 316L steel in chloride solution.

Keywords: chloride stress corrosion cracking; austenitic stainless steel

1. Introduction

One of the most accepted mechanisms of stress Corrosion cracking (SCC) (*i.e.*, the “dissolution-repassivation” mechanism [1–3]) requires recurrence of the steps of: (a) the stress-assisted disruption of the passive film at the crack-tip; (b) localized crack-tip dissolution at a high rate; and (c) repassivation at the crack-tip. Pitting is the one of the common SCC-initiators whereas the localized

crack-tip dissolution facilitates crack propagation. The development of a locally conducive electrochemistry can trigger and sustain pitting, whereas an intricate synergy of the local electrochemistry with an applied/residual tensile stress at the crack tip is essential for the corrosion-assisted propagation of cracks [4]. Therefore, both pitting and cracking can be extremely sensitive to variations in electrochemistry. For example, caustic crack propagation rate of a steel was reported [5,6] to be 25 times greater in a 3.5M caustic solution containing 0.4M sulphide than in the sulphide-free solution. However, the industrial practices for mitigation of pitting and assisted cracking are often developed on the basis of data generated in plain solutions, and minor but critical variations in solution chemistry are often ignored. Therefore, it is not surprising that the limited laboratory data on pitting/cracking susceptibility do not always corroborate the varied experience in processing plants.

The profound role of the environment chemistry in pitting/cracking susceptibility is relevant also for the incidents of the pitting and cracking of stripping columns for a polymer processing plant that were constructed from a few highly corrosion resistant alloys (viz., super duplex stainless steel, Incoloy 825 and 316L stainless steel). Most notably, pitting and cracking in this instance had initiated and/or accentuated particularly when a nitrite compound was used as an alternative chemical for arresting the polymerization reactions in the stripping step. Influence of addition of a few anion types (chromates, sulphates, molybdates and nitrates) to chloride solution on pitting and chloride cracking of stainless steels has been reported [7–15]. These investigations would suggest the addition of these anions to have an inhibiting effect in pitting of stainless steels.

A study by Newman and Ajjawi [8] on the influence of nitrate in growth of an artificial pit suggests that nitrate induces passivation under a salt film at certain potentials which depend on the nitrate-to-chloride ratio. In a subsequent study, Newman and Shahrabi [7] have suggested that the electro-reduction of nitrate anions may contribute to nitrogen enrichment on the active dissolution sites, improving pitting resistance. This model is consistent with the improvement in pitting resistance of nitrogen-bearing stainless steels. However, the considerable accentuation in pitting/cracking in the stripping column as a result of nitrite addition (described earlier) is not consistent with the reported inhibiting influence of nitrate. It may be pertinent also to refer to the authors' recent work [16] on SCC of a duplex stainless steel (DSS) in 30% MgCl₂ solutions at 180 °C, showing the nitrite addition to retard SCC susceptibility at 1400 and 2800 ppm but accelerate at 5600 ppm.

This paper presents results of slow strain rate testing of an austenitic stainless steel in chloride solutions with different levels of nitrite content.

2. Experimental

The test material (316L stainless steel) was received in rolled plate condition. Test samples were machined from the plates. The chemical composition (wt%) of 316L plates used in the present study is: C: 0.02, Cr: 16.6, Ni: 10.0, Mn: 1.69, Mo: 2.1, N: 0.04, Cu: 0.39, P: 0.03, Si: 0.39, Al: <0.001, S: 0.01, Fe: Balance. Microstructure of the duly polished steel surface was revealed by electrochemical etching (etchant: 10 wt. % oxalic acid, voltage: 20 V, current: 5 A, time: 100 s) and observed by optical microscopy.

Slow strain rate testing (SSRT) was employed for determination of SCC susceptibility. With the use of a variable speed motor, the SSRT rigs provide different constant cross-head speeds as the motor speed

is varied from 10% to 100% of the full motor speed, which corresponds to various strain rates in the range of 10^{-7} s $^{-1}$.

SSRT specimens were machined perpendicular to the rolling direction of the plate. Uniaxial cylindrical tensile specimens had an outer diameter (OD) of 8.0 ± 0.2 mm, with a gauge section of 20.0 ± 0.2 mm length and 3.0 ± 0.2 mm OD. The gauge section was ground in the longitudinal direction progressively to a 1200 grit finish, rinsed with acetone/water and air dried. A layer of Teflon tape was applied on the specimens except for their gauge sections. However, special care was taken while applying the tape to ensure there was no crevice corrosion. After a final rinse with acetone, the specimen was immediately mounted into the corrosion vessel which was then filled with different test solutions at 150 °C. While 30 wt. % MgCl $_2$ ($\sim 2.23 \times 10^5$ ppm Cl $^-$) constituted the primary test solution, some of the tests solutions were added with various concentrations of nitrite (in ppm by weight), in order to achieve different chloride-to-nitrite ratios, as described in Table 1. All solutions were prepared using laboratory grade chemicals and distilled water.

Table 1. Solutions used for electrochemical experiments to characterize the effects of nitrite anions.

Volume of 1 M NaNO $_2$ added to 250 mL 30 wt. % MgCl $_2$	Concentration of NO $_2^-$ anions (ppm)
0	0
10	1400
20	2800
40	5600

While immersed in the test solution and subjected to straining at a constant rate, tensile stress was measured using a load cell and recorded every 10 min by a data-taker. All tests were conducted under open circuit potential conditions and the tensile specimen insulated from the grips and autoclave body by using appropriate Teflon and ceramic insulators. Fractographic examinations of specimens after completion of SSRT tests were carried out using scanning electron microscopy (SEM) in order to investigate the fractographic features of SCC.

For understanding the electrochemical influence of nitrite addition, a few anodic polarization runs were also carried out, using a typical three-electrode system and a Princeton Applied Research (PAR) 273 potentiostat. An external saturated calomel reference electrode (SCE) was used in conjunction with a fine-sinter glass luggin while a single graphite rod was used as the counter electrode. The working electrode consisted of machined cylindrical rods of approximately 30 mm in length and 8 mm outer diameter (OD). A wetted surface area of approximately 0.19 cm 2 was defined as the area tested. Prior to installation in the corrosion cell, the working electrode end was wet ground with silicon carbide paper to a 1200 grit finish, rinsed with distilled water followed by a degreasing rinse with acetone and subsequently air-dried. The test solution consisted of 150 mL 0.1M NaCl mixed with varying volumes of 0.1M sodium nitrate (NaNO $_3$). The desired temperature of the working solution was set and maintained for the duration of the experiment. All solutions were prepared from analytical grade reagents and distilled water, and were used in their naturally aerated state. Prior to every polarisation scan, a 30 s period of conditioning at -1.00 V was performed to remove the passive layer on the alloy surface. After conditioning, a delay of two hours allowed for open circuit potential (OCP) stabilisation. All scans

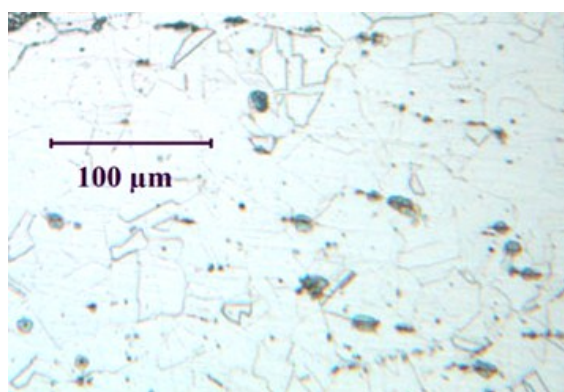
were started at -250 mV (with respect to OCP) and continued onwards to the anodic region until the onset of transpassivity.

3. Results and Discussion

The etched microstructure of the 316L stainless steel (shown in Figure 1) consists primarily of austenite grains.

Two sets of slow strain rate testing (SSRT) experiments were carried out, the first set for identifying the strain rate or the range of strain rates that produces SCC in plain 30% MgCl_2 solution, and the second set for comparison of SCC susceptibility in 30% MgCl_2 , with and without nitrite addition (at a strain rate as identified through the first set of experiments).

Figure 1. Etched microstructure of 316L stainless steel used in the present study.



3.1. SSRT in Plain MgCl_2 Solution at Various Strain Rates

Figure 2 presents the force vs. time curves for the SSRT specimens tested at 150 °C at 30%, 40%, 50% and 70% of the full motor speed, which respectively correspond to the strain rates of 3.7×10^{-7} , 5.3×10^{-7} , 6.7×10^{-7} and $10.6 \times 10^{-7} \text{ s}^{-1}$. It is evident from Figure 2 that time to failure (t_f) is considerably lower at 3.7×10^{-7} , 5.3×10^{-7} , $6.7 \times 10^{-7} \text{ s}^{-1}$ in comparison to that at $10.6 \times 10^{-7} \text{ s}^{-1}$. While the shorter t_f at $10.6 \times 10^{-7} \text{ s}^{-1}$ may simply be attributed to the strain rate, the considerably longer t_f for the specimen tested at $6.7 \times 10^{-7} \text{ s}^{-1}$ in comparison to the specimen tested at 3.7×10^{-7} and $5.3 \times 10^{-7} \text{ s}^{-1}$ is a strong indication of SCC at 3.7×10^{-7} and $5.3 \times 10^{-7} \text{ s}^{-1}$. Indeed, the SEM fractography revealed the features of intergranular SCC (Figure 3) on a considerable fraction of the fracture surfaces of specimens tested at 3.7×10^{-7} and $5.3 \times 10^{-7} \text{ s}^{-1}$. The remainder of the fracture surfaces of these specimens had features indicative of only mechanical failure (*i.e.*, ductile dimples, as shown in Figure 4). On the other hand, the entire fracture surface of the specimens tested at 6.7×10^{-7} and $10.6 \times 10^{-7} \text{ s}^{-1}$ only had ductile dimples (similar to the features shown in Figure 4), *i.e.*, no areas with features of intergranular cracking were detected on these specimens. These results suggest the strain rates of $3.7 \times 10^{-7} \text{ s}^{-1}$ and $5.3 \times 10^{-7} \text{ s}^{-1}$ to be suitable for causing intergranular cracking to 316L immersed in 30% MgCl_2 at 150 °C.

Figure 2. Force vs. time slow strain rate testing (SSRT) curves of 316L in 30 wt. % MgCl₂ at 150 °C, at different strain rates.

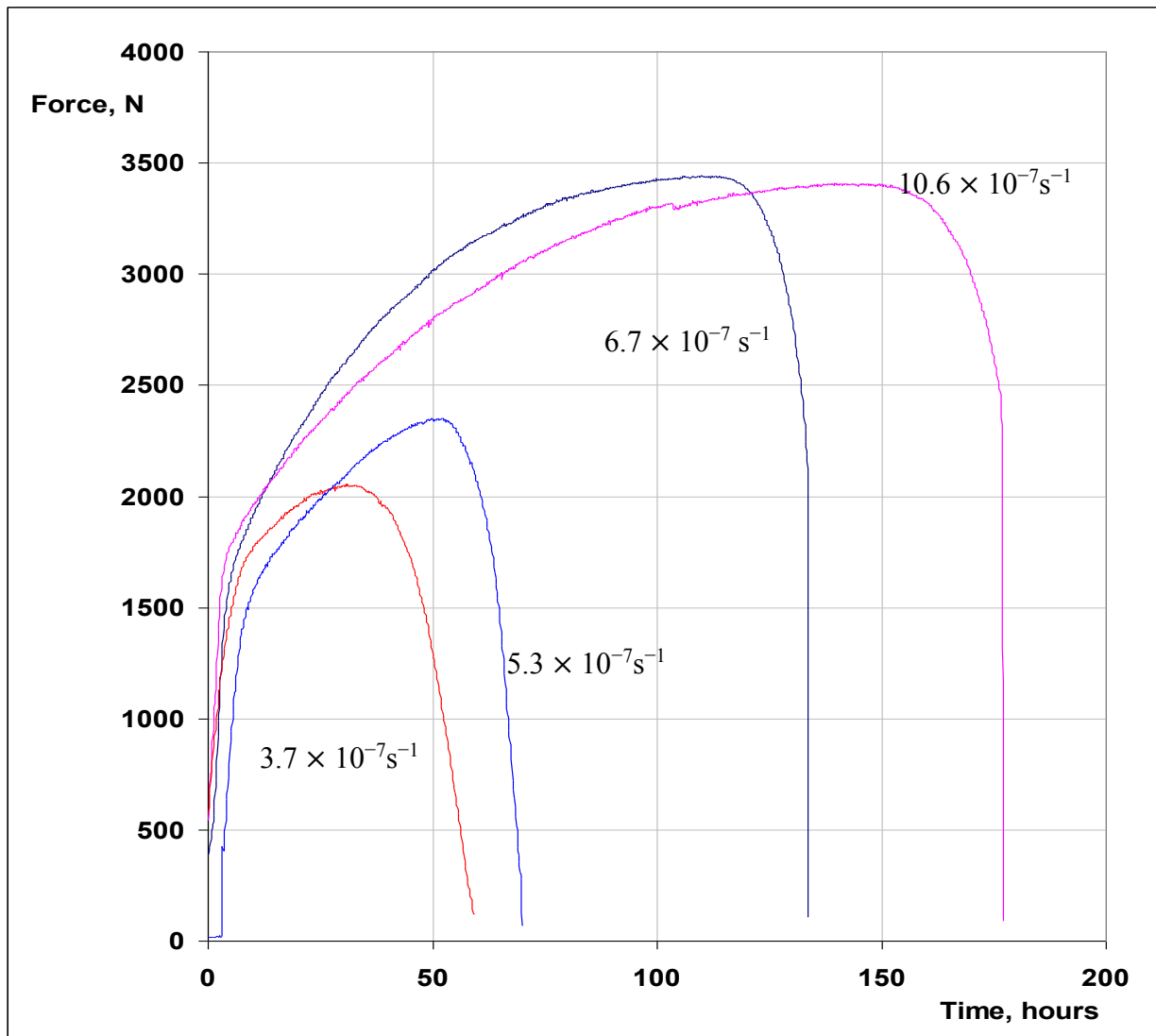


Figure 3. SEM fractograph of 316L tested in 30 wt. % MgCl₂ at 150 °C, showing intergranular stress corrosion cracking (SCC) that covered a considerable fraction of the fracture surface, when tested at strain rates: (a) $3.7 \times 10^{-7} s^{-1}$ and (b) $5.3 \times 10^{-7} s^{-1}$.

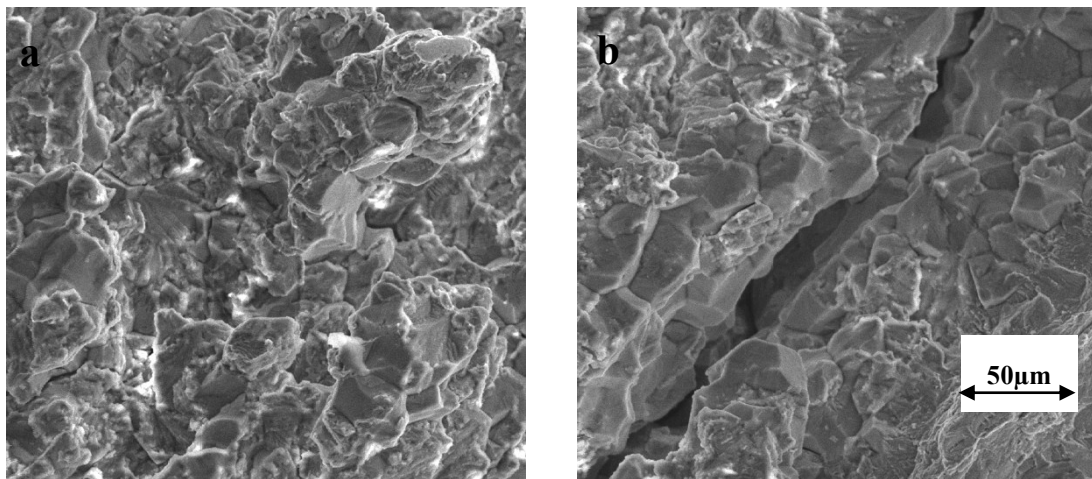
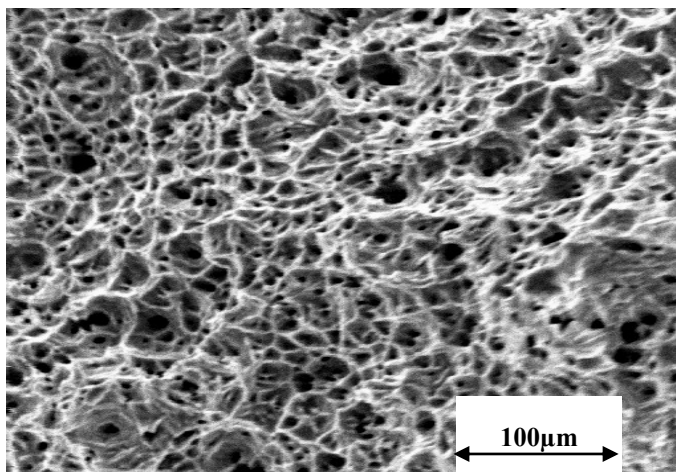


Figure 4. A representative SEM fractograph showing purely ductile failure.



3.2. SSRT in Nitrite-Containing MgCl₂ Solution

SSRT runs carried out using plain 30 wt. % MgCl₂ solution at 150 °C have clearly resulted in intergranular SCC when strain rates of $3.7 \times 10^{-7} \text{ s}^{-1}$ and $5.3 \times 10^{-7} \text{ s}^{-1}$ were employed (as reported in Section 3.1). Accordingly, all SSRT tests for investigating the role of nitrite addition to the 30 wt. % MgCl₂ solution were carried out only at $3.7 \times 10^{-7} \text{ s}^{-1}$.

Figure 5 presents the force *versus* time curves for SSRT specimens tested in the plain MgCl₂ solution as well as in the MgCl₂ solution with the addition of 1400, 2800 and 5600 ppm (by wt.) of NO₂⁻ anions. Intergranular cracking (Figure 6a) and transgranular cracking (Figure 6b), as shown in the representative SEM fractographs confirm the presence of SCC in each case. The addition of NO₂⁻ to the chloride solution clearly accelerates the SCC failure. The SSRT plots show a systematic increase in SCC-susceptibility with increase in NO₂⁻ content, as indicated by the systematic increase in t_f with decreasing NO₂⁻, *i.e.*, 5600 ppm > 2800 ppm > 1400 ppm (Figure 5). Maximum force sustained was also considerably lower in the case of specimens tested in solutions with 2800 and 5600 ppm NO₂⁻. SEM fractography has also suggested that while the samples tested in solutions with 0, 1400 and 2800 ppm NO₂⁻ produced only intergranular SCC (Figure 6a), the fractographs of the samples tested in solutions with 5600 ppm NO₂⁻ also had significant areas of trans-granular SCC (in addition to intergranular SCC), as shown in Figure 6b.

The increase in SCC susceptibility with the nitrite addition (Figure 5) may be attributed to the ability of the nitrite contents used in this study to provide just enough passivation that may be necessary for sustaining the stress corrosion cracking. It may be rudimentary but still very relevant to recall here that a relatively less stable passive film would facilitate the sustenance of the SCC (for the systems susceptible to SCC by dissolution-repassivation mechanism).

This effect appears to increase with increasing nitrite content in the range of 1400–5600 ppm. A few anodic polarization tests using solutions with 1400, 2800 and 5600 ppm of NO₂⁻ (Figure 7) suggest extensive meta-stable pitting activity in the solution with no NO₂⁻, and a systematic decrease in the activity with increasing NO₂⁻ content. Also, a systematically increasing positive shift in pitting potential was observed with the increase in the NO₂⁻ content. There is very little meta-stable pitting activity in the case of solution with 5600 ppm of NO₂⁻, which may indicate a significant role of the pitting-independent

SCC mechanism at high NO_2^- contents. With increasing passivation characteristic upon increase in NO_2^- content of the solution, a condition may establish for cracks to initiate and propagate also within grains (*i.e.*, trans-granular cracking), *i.e.*, without the need of grain boundary pitting. Of the solutions used, this aspect will be facilitated most in the solution with 5600 ppm NO_2^- and hence the considerable area of trans-granular cracking (Figure 6b). Thus the initiation of stress corrosion cracks does not need to rely on grain boundary pitting, which is consistent with the enhanced SCC with increasing NO_2^- addition.

Figure 5. Force vs. Time SSRT curves (at strain rate of $3.7 \times 10^{-7} \text{ s}^{-1}$) for 316L in 30 wt. % MgCl_2 at 150 °C, with different concentrations of NO_2^- .

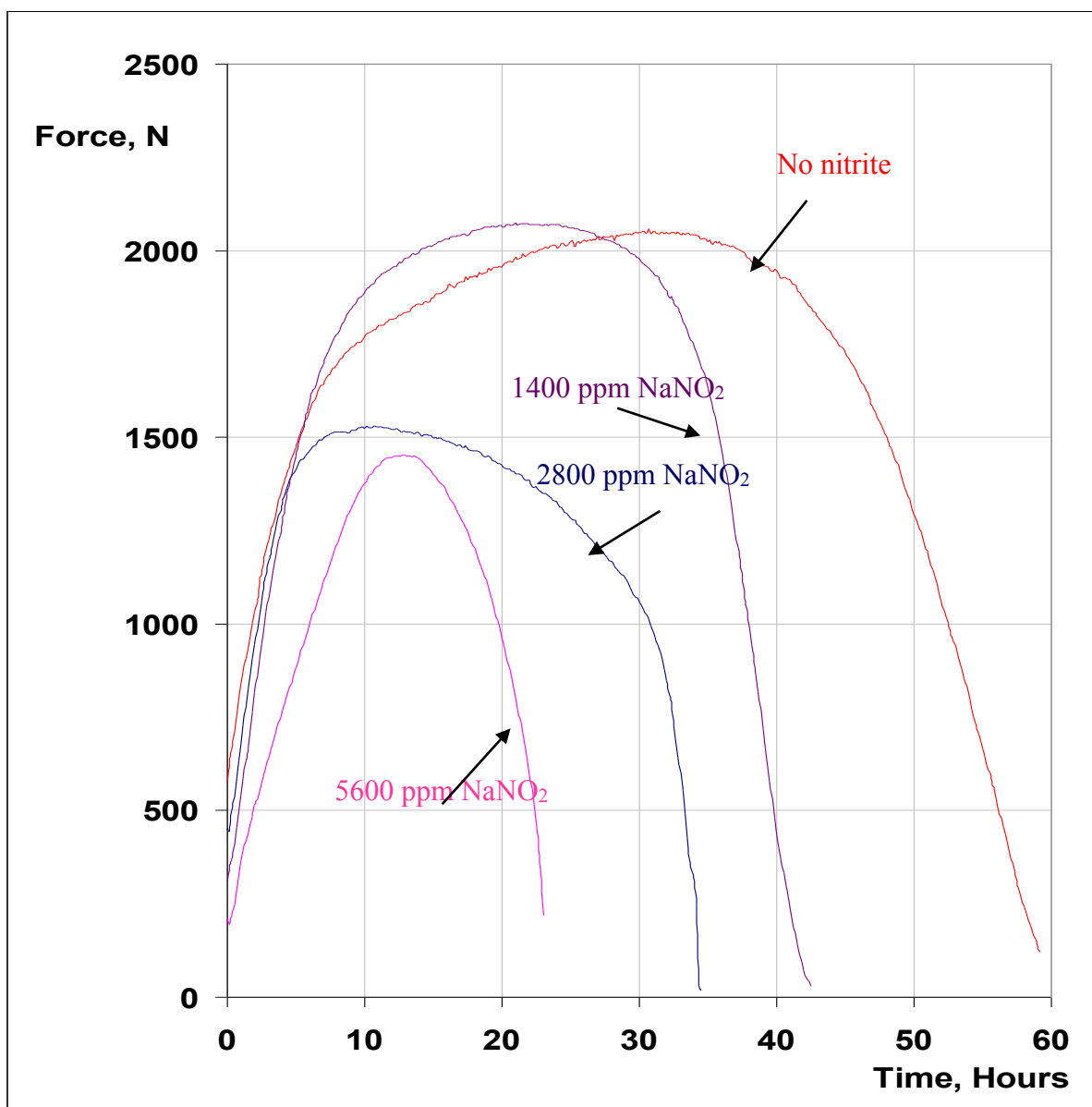


Figure 6. SEM fractograph of 316L tested in 30 wt. % MgCl₂ at 150 °C at $3.7 \times 10^{-7} \text{ s}^{-1}$, showing: (a) intergranular SCC (IGSCC) in solution with 0, 1400 and 2800 ppm NO₂⁻, and (b) trans-granular SCC (in addition to IGSCC) in solution with 5600 ppm NO₂⁻.

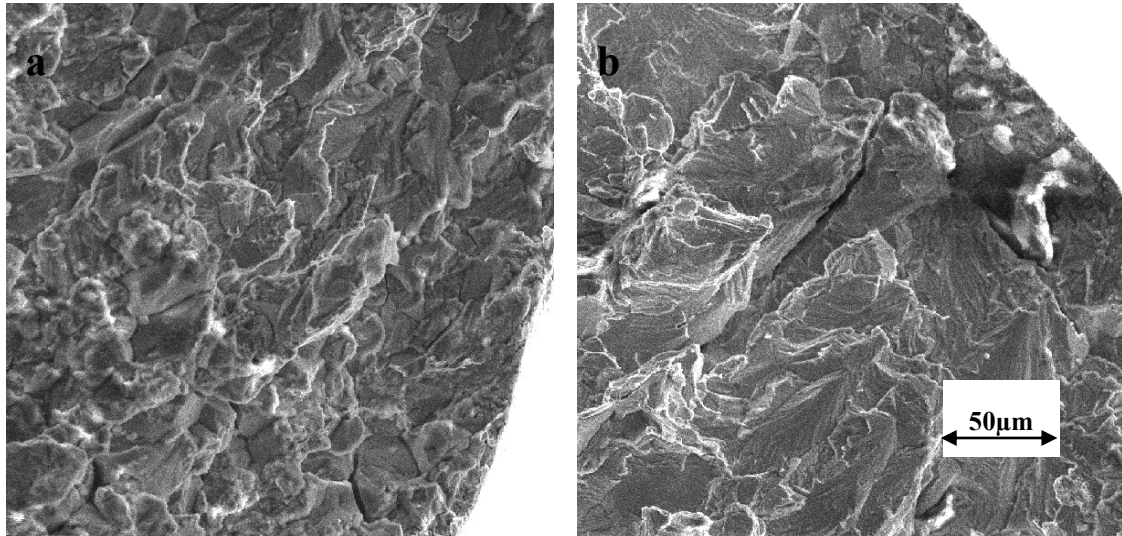
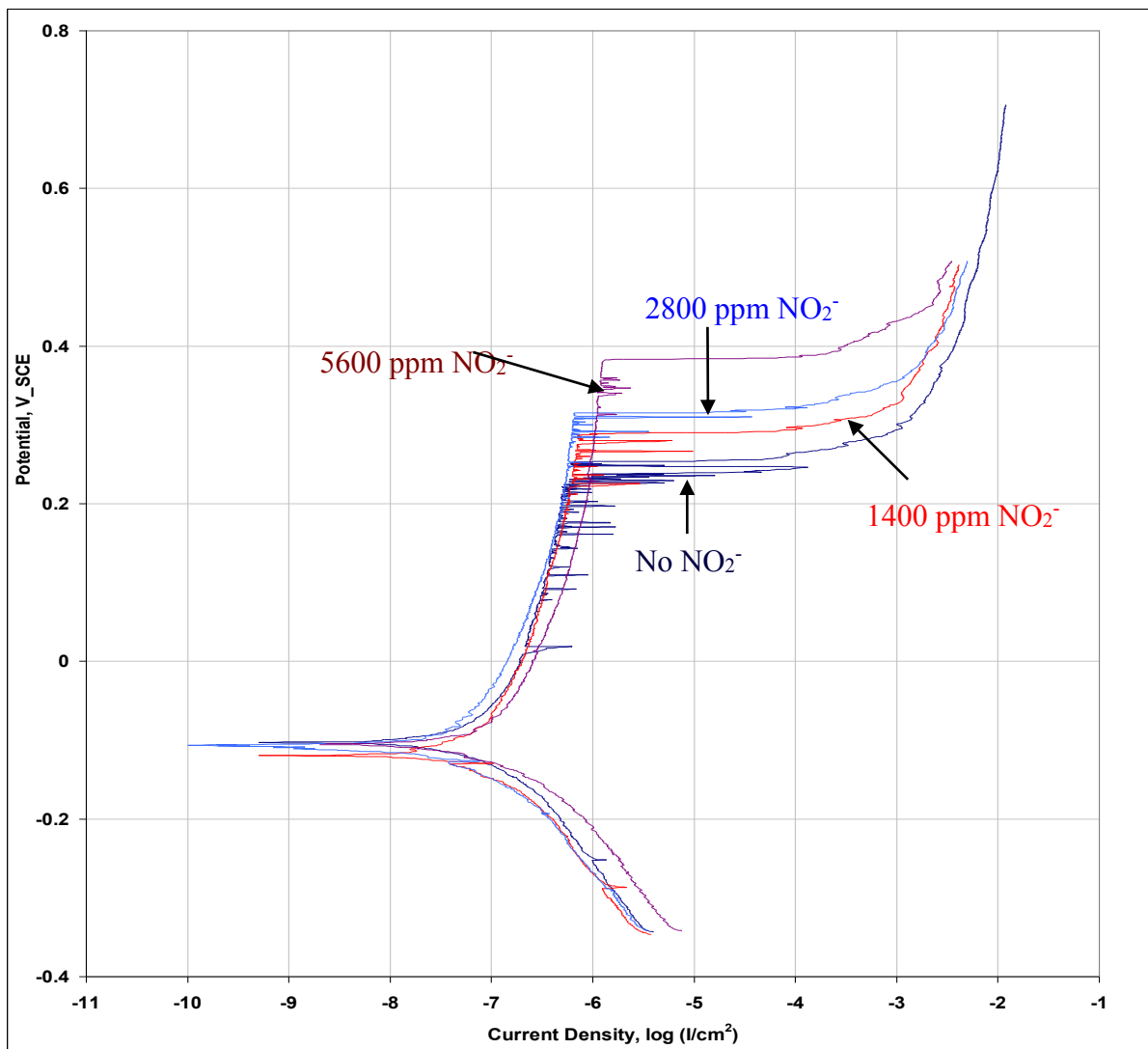


Figure 7. Anodic polarization curves of 316L in 0.1M NaCl with 0, 1400, 2800, and 5600 ppm NO₂⁻.



The authors' own work [16] on SCC of a duplex stainless steel (DSS), SAF 2507 in 30% MgCl₂ solutions at 180 °C has suggested the nitrite addition to retard SCC susceptibility at 1400 and 2800 ppm. This behaviour is possibly a result of the much superior passivation characteristics and greater resistance to SCC and pitting (as a result of its greater Cr content and the dual phase structure of DSS). The electrochemical tests reported in the same paper [16] have shown that with the addition of 1400 and 2800 ppm NO₂⁻ a robust passive layer develops, which resists its own cracking as well as SCC. Accordingly, it is believed that a much higher NO₂⁻ content may be required for developing such a robust layer in the case 316L SS.

4. Conclusions

As established by slow strain rate testing (SSRT) of 316L stainless steel at various strain rates in 30% MagCl₂ solution at 150 °C, with and without various NO₂⁻ additions, and by the post-SSRT fractography:

- (a) 316L suffers intergranular stress corrosion cracking (SCC) at strain rates of 3.7×10^{-7} and $5.3 \times 10^{-7} \text{ s}^{-1}$, and no SCC at higher strain rates.
- (b) Additions of NO₂⁻ (1400–5600 ppm) accelerate susceptibility to chloride SCC.
- (c) With increasing NO₂⁻ content, SCC susceptibility increases in the order, 1400 ppm > 2800 ppm > 5600 ppm. This behaviour has been attributed to the increasing passivation characteristic with increasing NO₂⁻ content.

Acknowledgments

Authors are grateful to the Australian Research Council for a Linkage Grant, which enabled the work presented in this paper.

Author Contributions

Both the authors have contributed equally to the work reported in this article. Singh and Siew together conceptualized and planned the work, Siew carried out the experimental work whereas Singh was responsible for developing the manuscript.

Conflicts of Interest

The authors declare no conflict of interest.

References

1. Jones, D.A. *Principles & Prevention of Corrosion*, 2nd ed.; Prentice Hall: Upper Saddle River, NJ, USA, 1992; p. 239.
2. Singh Raman, R.K.; Saxena, A. Role of imposed potential in expanding the regime of strain rates for caustic cracking. *J. Electrochem. Soc.* **2007**, *154*, C451–C457.
3. Singh Raman, R.K. Evaluation of caustic embrittlement susceptibility of steels by slow strain rate testing. *Metall. Mater. Trans. A* **2005**, *36A*, 1817–1823.

4. Singh Raman, R.K. Role of caustic concentration and electrochemical potentials in caustic cracking of steels. *Mater. Sci. Eng. A* **2006**, *441*, 342–348.
5. Singbeil, D.; Tromans, D.J. Effect of sulfide ions on caustic cracking of mild steel. *Electrochem. Soc. Electrochem. Sci. Technol. Corros.* **1981**, *128*, 2065–2070.
6. Singbeil, D.; Tromans, D.J. Caustic stress corrosion cracking of mild steel. *Metall. Trans. A* **1982**, *13*, 1091–1098.
7. Newman, R.C.; Shahrabi, T. The effect of alloyed nitrogen or dissolved nitrate ions on the anodic behaviour of austenitic stainless steel in hydrochloric acid. *Corros. Sci.* **1987**, *27*, 827–838.
8. Newman, R.C.; Ajjawi, M.A. A micro-electrode study of the nitrate effect on pitting of stainless steels. *Corros. Sci.* **1986**, *26*, 1057–1063.
9. Zuo, Y.; Wang, H.; Zhao, J.; Xiong, J. The effects of some anions on metastable pitting of 316L stainless steel. *Corros. Sci.* **2002**, *44*, 13–24.
10. Uhlig, H.H.; Cook, E.W., Jr. Mechanism of inhibiting stress corrosion cracking of 18-8 stainless steel in MgCl_2 by acetates and nitrates. *J. Electrochem. Soc.* **1969**, *116*, 173–177.
11. Leckie, H.P.; Uhlig, H.H. Environmental factors affecting the critical potential for pitting in 18–8 stainless steel. *J. Electrochem. Soc.* **1966**, *113*, 1262–1267.
12. Jones, R.L. Nitrate effects promoting the stress corrosion cracking of AISI type 304 stainless steel in MgCl_2 Above 200 °C. *Corrosion* **1975**, *31*, 431–434.
13. Illevbare, G.O.; King, K.J.; Gordon, S.R.; Elayat, H.A.; Gdowski, G.E.; Summers, T.S.E. Effect of nitrate on the repassivation potential of alloy 22 in chloride containing environments, In Proceedings of the 206th Meeting of The Electrochemical Society, Honolulu, HI, USA, 3–8 October 2004.
14. Refaey, S.A.M.; el-Rehim, S.S.A.; Taha, F.; Saleh, M.B.; Ahmed, R.A. Inhibition of chloride localized corrosion of mild steel by PO_4^{3-} , CrO_4^{2-} , MoO_4^{2-} , and NO_2^- anions. *Appl. Surface Sci.* **2000**, *158*, 190–196.
15. Bardwell, J.A.; Sproule, G.I.; Mitchell, D.F.; Macdougall, B.; Graham, M.J. Nature of the passive film on Fe–Cr alloys as studied by ^{18}O secondary ion mass spectrometry: reduction of the prior film and stability to *ex-situ* surface analysis. *J. Chem. Soc. Faraday Trans.* **1991**, *87*, 1011–1019.
16. Singh Raman, R.K.; Siew, W.H. Role of nitrite addition in chloride stress corrosion cracking of a super duplex stainless steel. *Corros. Sci.* **2010**, *52*, 113–117.